3rd URSI AT-AP-RASC, Gran Canaria, 29 May – 3 June 2022

Calculation of Ionospheric Disturbances of Earthquakes in Europe with TEC Anomalies

M. Baran Ökten*(1)(2), Zehra Can(3), Ö. Faruk Aydın(3), Almina Dokur(3), and Anjelika Aydın(3)
(1) Yildiz Technical University, Faculty of Chemical and Metallurgical Engineering, Metallurgical and Materials Engineering, Istanbul, Turkey, 34220, l5418047@std.yildiz.edu.tr
(2) TUBITAK Polar Research Institute, Kocaeli, Turkey, 41470, http://tubitak.gov.tr
(3) Yildiz Technical University, Faculty of Art and Sciences, Department of Physics, Istanbul, Turkey, 34220,

Abstract

The Earth's ionosphere, which is a natural plasma, can be affected by many factors such as spacecraft launches, explosions in mines, energy fluctuations created by nuclear tests that will cause energy release, solar geomagnetic storms, and seismic activities. Total Electron Content (TEC) is among the most practical ways to study these disturbations. Significant changes occur in the TEC value, especially before and after large earthquakes. For this reason, it is of great importance to examine the anomalies created by earthquakes to establish the lithosphere-ionosphere connection more clearly. In this study, the TEC anomalies 15 days before and 15 days after the earthquakes of 6 and above in the European continent between 2010 and 2020 were calculated using the data obtained from the GIRO ionosondes located in an imaginary circle formed by the earthquake strain radius and analyzed in the heat map collectively. In this way, the ionospheric anomalies caused by all the examined earthquakes could be analyzed clearly on a daily and hourly basis. In particular, it has been determined that negative anomalies start in the evening hours of twelve days before the earthquakes and last until the morning, and positive anomalies increase two days before the earthquake. Anomalies were identified eight days before the earthquake and were large and prolonged. It was determined that positive anomalies appeared four days after the earthquake.

1. Introduction

Ionospheric disturbances occur due to many factors because the Earth's ionosphere, which is a natural plasma, has a structure that changes according to the season, time of day, and geographical location. Solar wind plasma, geomagnetic storms, seismic activities that occur during the earthquake process can be counted among the reasons for this confusion. The first research on ionospheric disturbances caused by large earthquakes was done by Leonard and Barnes. Leonard and Barnes investigated the ionospheric disturbances during the Alaska earthquake with the ionogram obtained from ionosondes in Alaska [1]. Fuying et al. investigated the statistical analysis of pre-earthquake ionospheric TEC anomalies using GPS TEC data and determined that ionospheric TEC showed significant increases and decreases for 50 earthquakes with $\mathrm{Mw} \geq 7$. After eliminating the changes caused by geomagnetic activity, they detected significant increases and decreases in the ionospheric TEC value before 94% of all earthquakes they examined. They stated that TEC reduction occurred approximately one week before the earthquake [2].

Pulinets et al. showed that radon gas, which emerged from the fractured areas due to the mobility in the Earth's crust, spread to the Earth together with gases such as carbon dioxide, methane, hydrogen, and helium [3]. The resulting diffusion process increases the conductivity of the boundary layer by activating atmospheric ionization. The increase in ion concentration creates ion clusters and changes the air conductivity [3-5]. Boundary potential, the differential potential between ionosphere and soil, and the relationship between positive TEC anomaly and negative TEC anomaly have been explained in great detail in studies [3-5]. As follows, in conditions of high ionization level, relative humidity creates large ion clusters. Calm weather, on the other hand, causes large aerosol-sized heavy-ion clusters to form easily. If the boundary potential is greater than the differential potential between the ionosphere and the soil, heavy ions dominate at the boundary of the atmosphere. The abundance of heavy ions, on the other hand, significantly reduces the air conductivity and increases the ionospheric potential. As a result, positive ionospheric anomalies occur before the major earthquakes. If the boundary potential is smaller than the differential potential, the conductivity of the atmosphere increases, causing the ionospheric potential to decrease relative to the ground. Therefore, negative ionospheric anomalies can be observed before major earthquakes. İyonizasyon etkisinin gelişme sürecinden, radon akı artışının erken aşamalarında aktif olan deprem bölgesi üzerinde elektron konsantrasyonunun negatif sapması tespit edilebilir [3-5].

Guo et al., in their study, determined the TEC anomaly that lasted for about six hours during the Iquique Earthquake of April 1, 2014, and emphasized that the theory proposed by Pulinets was reliable [5].

Dobrovolsky, assuming that the effective manifestation zone of the deformations that will be created by an earthquake is a circle in which the epicenter of the prepared earthquake is taken as the center, and that this radius is; showed that it is a function of the earthquake magnitude and that these theoretical results are in satisfactory agreement with the field results [6]. This radius, called 'strain radius', is calculated in kilometers as follows,

$$r = 10^{0,43M} \quad (1)$$

M is the magnitude of the earthquake.

In this study, earthquakes of 6 and above magnitudes between 2010 and 2020 in the Ionospheric Mid-Latitude Regions of the European Continent, which have similar ionospheric characteristics with Turkey, were determined. For these earthquakes, TEC data were obtained by determining the ionosondes in the regions within the strain radius circle, stations with more than 75% reliable data among these ionosondes, and TEC anomalies were detected 15 days before and after the earthquakes. Geomagnetic storm data were also analyzed to determine whether the TEC anomaly is due to an earthquake or a geomagnetic storm.

2. Data and Methodology

2.1 Data

Network data from the global digital ionosonde provided by the Global Ionospheric Radio Observatory (GIRO) were used in this research. GIRO makes it possible and easier to reach ionospheric plasma measurement values [7]. GIRO is a vital data provider for ionosphere and space weather studies. Ionospheric data retrieved from giro.uml.edu. The TEC data obtained from the ionosondes in the earthquake preparedness zone were evaluated by taking into account the solar geomagnetic conditions. For geomagnetic storm analysis, the Dst index was obtained from wdc.kugi.kyoto-u.ac.jp website, and the Kp index and the F10.7 solar flux values were obtained from omniweb.gsfc.nasa.gov website. Basic information about earthquakes was taken from the United States Geological Survey (USGS). The open-source https://github.com/jupyter-widgets/ipyleaflet library was used for drawing the map, data visualizations, and 2D visualizations in Figure 1.

2.2 Methodology

Earthquakes with a magnitude of Mw ≥6 that occurred in the European Continent between 2010-2020 were detected, and the ionospheric effects of these earthquakes were examined through TEC data by selecting those with data above 75% among the ionospheric stations within the strain radius calculated in the Equation 1. The earthquakes and the ionosonde stations are shown in Figure 1.

Information about the existence of geomagnetic storms was obtained by examining the Dst and F10.7 Solar Flux values on the examined dates.
The earthquakes in question are given in Table 1. along with various information such as the city where they occurred, depth, magnitude, strain radius.

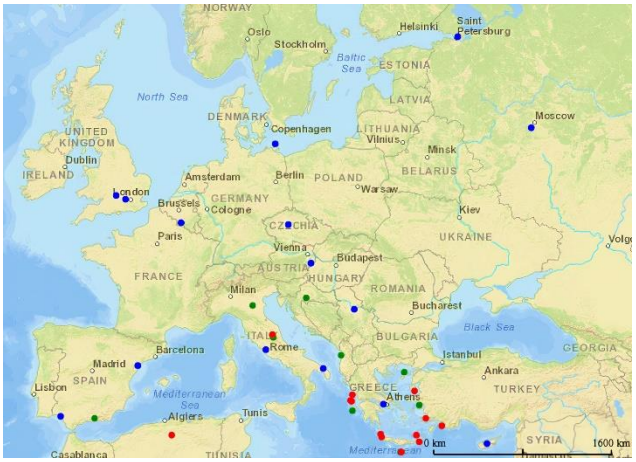

Figure 1. Map of Mw>6 earthquakes occurring in Continental Europe between 2010 and 2020, earthquakes with (shown in green) and without (shown in red) more than 75% reliable TEC data in the strain radius and GIRO ionosondes (shown in blue). The map was drawn using https://github.com/jupyter-widgets/ipyleaflet.

TEC is a parameter that expresses the properties of the ionosphere and is used to study the structure of the ionosphere. It is equal to the line integral of the electron density.

$$TEC = \int N_e dl \quad (2)$$

The unit of TEC, which is also interpreted as the total amount of free electrons along with a cylinder with a cross-section of square meter, is TECU, which is 10^{16} electrons/m^2 [8].

Since TEC is a measure of the number of free electrons, it reaches its highest level around 14:00 local time and vice versa, since electrons are also excited by the solar radiation of molecules in the atmosphere during the daytime; TEC decreases at night as electrons combine with ions. One should also note that the variation in TEC varies with seasons and geographic latitudes.For the calculation of TEC Anomalies, TEC data of stations in the Strain radius region were downloaded from thirty days before to fifteen days after the earthquake. To equalize their resolution, since most of the stations used have a resolution of fifteen minutes; different resolutions was reduced to fifteen minutes by the averaging them. A path similar to the Quarterly Span method adopted by Liu et al. was chosen to identify anomalies [9].

For consecutive hours; the averages of fifteen consecutive days, the upper and lower quartiles were calculated and the upper and lower limits were calculated by,

$$\begin{cases} TEC_{Up} = TEC_{Av} + 1{,}5\left(TEC_{UQ} - TEC_{Av}\right) \\ TEC_{Low} = TEC_{Av} - 1{,}5\left(TEC_{Av} - TEC_{LQ}\right) \end{cases} \quad (3)$$

where TEC_{Up} , TEC_{Low} , TEC_{Av} , TEC_{UQ} and TEC_{LQ} are upper bound, lower bound, average, upper quartile and lower quartile of TEC data series, respectively. Ergo, the anomalies are also calculated as follows,

$$\begin{cases} \Delta TEC_P = TEC - TEC_{Up}, & TEC > TEC_{Up} \\ \Delta TEC_N = TEC - TEC_{Low}, & TEC < TEC_{Low} \end{cases} \quad (4)$$

Where ΔTEC_P is positive and ΔTEC_N is negative anomaly. In other words, if TEC is lower than the lower limit, we call the difference as negative anomaly, and if it is greater than the upper limit, we call it positive anomaly. Since TEC differs from region to season according to many different variables, we found it more appropriate to analyze the anomaly by considering the size of the anomaly compared to the normal conditions of the study environment.

Table 1. Dates, times, coordinates, magnitudes, and radius of the earthquake preparation zone calculated according to Eq. 1. Analyzed earthquakes are indicated with an asterisk.

Name	Date (DD-MM-YYYY)	Time (UTC)	Latitude (°)	Longitude (°)	Magnitude (Mw)	Depth (km)	Strain Radius (km)
Nigüelas, Spain*	11.04.2010	22:08:12	36,97	3,54	6,3	609,8	511,68
Crete, Greece	1.04.2011	13:29:10	35,66	26,56	6,0	59,9	380,19
Emilia, Italy*	20.05.2012	02:03:52	44,89	11,23	6,0	6,3	380,19
Dodecanese Islands, Greece	10.06.2012	12:44:16	36,42	28,88	6,0	35,0	380,19
Pýrgos, Greece*	15.06.2013	16:11:02	34,40	25,02	6,2	10,0	463,45
Pýrgos, Greece*	16.06.2013	21:39:05	34,35	25,16	6,0	19,0	380,19
Platanos, Greece	12.10.2013	13:11:53	35,51	23,25	6,6	40,0	688,65
Lixoúri, Greece	26.01.2014	13:55:42	38,21	20,45	6,1	8,0	419,76
Lixoúri, Greece	3.02.2014	03:08:46	38,26	20,39	6,0	5,0	380,19
Kamariótissa, Greece*	24.05.2014	09:25:02	40,29	25,39	6,9	6,4	926,83
Fry, Greece	16.04.2015	18:07:43	35,19	26,82	6,0	20,0	380,19
Lefkáda, Greece	17.11.2015	07:10:07	38,67	20,60	6,5	11,0	623,73
Al Hoceïma, Morocco	25.01.2016	04:22:02	35,65	3,68	6,3	12,0	511,68
Accumoli, Italy*	24.08.2016	01:36:32	42,72	13,19	6,2	4,4	463,45
Visso, Italy*	26.10.2016	19:18:08	42,96	13,07	6,1	10,0	419,76
Preci, Italy*	30.10.2016	06:40:18	42,86	13,10	6,6	8,0	688,65
Plomári, Greece	12.06.2017	12:28:39	38,93	26,37	6,3	12,0	511,68
Kos, Greece	20.07.2017	22:31:11	36,93	27,41	6,6	7,0	688,65
Lithakiá, Greece*	25.10.2018	22:54:52	37,52	20,56	6,8	14,0	839,46
Mamurras, Albania*	26.11.2019	02:54:12	41,51	19,53	6,4	22,0	564,94
Kissamos, Greece	27.11.2019	07:23:42	35,72	23,23	6,0	69,0	380,19
Néon Karlovásion, Greece*	30.10.2020	11:51:27	37,90	26,78	7,0	21,0	1023,29
Petrinja, Croatia*	29.12.2020	11:19:54	45,42	16,26	6,4	10,0	564,94

By dividing the anomaly we found by the mean and multiplying by hundred as show below,

$$\frac{\Delta TEC}{TEC_{Av}} \times 100\% \quad (5)$$

we have obtained the percent anomaly ratio. We have shown the average of the anomaly rates we found for consecutive times for all the earthquakes studied, with the temperature on the y-axis and UTC time on the x-axis in the temperature graph given in Figure 2 for the 13 days before and after the earthquake. Thus, by examining earthquakes, collectively; We can make interpretations such as day or night about the time of occurrence of anomalies.

3. Analysis

Negative anomalies can be seen in the evening, twelve days before the earthquake. The size and length of the anomalies increase as the earthquake day approaches. Six days before the earthquake until the day of the earthquake, between 02.00 and 04.00 (UT), short-term but large positive anomalies appear in addition to the negative anomalies and are replaced by positive anomalies again. The magnitude of these positive anomalies decreases as the day of the earthquake approaches and, they appear smaller and later after the day of the earthquake. Negative anomalies, which start in the evening and continue until the morning, start to be seen as large and long-lasting eight days before the earthquake, even though they start twelve days before the earthquake.

On days with large positive anomalies at midnight, weak negative anomalies are also seen at noon. In addition, the positive anomaly that occurred between 17:30 and 18:00, six days before the earthquake, is particularly striking. Two days before the earthquake, the mentioned afternoon anomalies start to decrease gradually. On the morning of the day before the earthquakes, unlike the previous days; this time there are positive anomalies. In the evening, the weak negative anomalies start again.

Although singular but large anomalies can be mentioned on the day of the earthquake, each earthquake should be analyzed separately so that a clear interpretation can be made about the day of the earthquake. The day after the earthquake, between midnight and morning; There is a partially large negative anomaly between two large positive anomalies. From four days after the earthquake to ten days after the earthquake, positive anomalies start at 04:00 and last until 18:00.

4. Conclusions

As can be seen, there are anomalies, especially from the twelve days before the earthquake to the eight days after the earthquake. The majority of anomalies before the earthquake are negative and occur between 17.00 and 06.00. After the earthquake, positive anomalies are intense. Again, by examining air conductivity and TEC anomalies together, it will be useful to establish the relationship between the differential potential between the ionosphere and the soil.

Although it can be concluded from the results that before the earthquake, the boundary potential is smaller than the differential potential, it tends to increase after the earthquake, but examining the atmospheric conductivity data can provide a clearer interpretation. In future studies, different properties of the ionosphere layers such as maximum heights, slab thickness, and critical frequencies can be investigated. By carrying out similar studies in different regions for similar and different years, a clearer understanding of the responses of regions to earthquakes can be achieved.

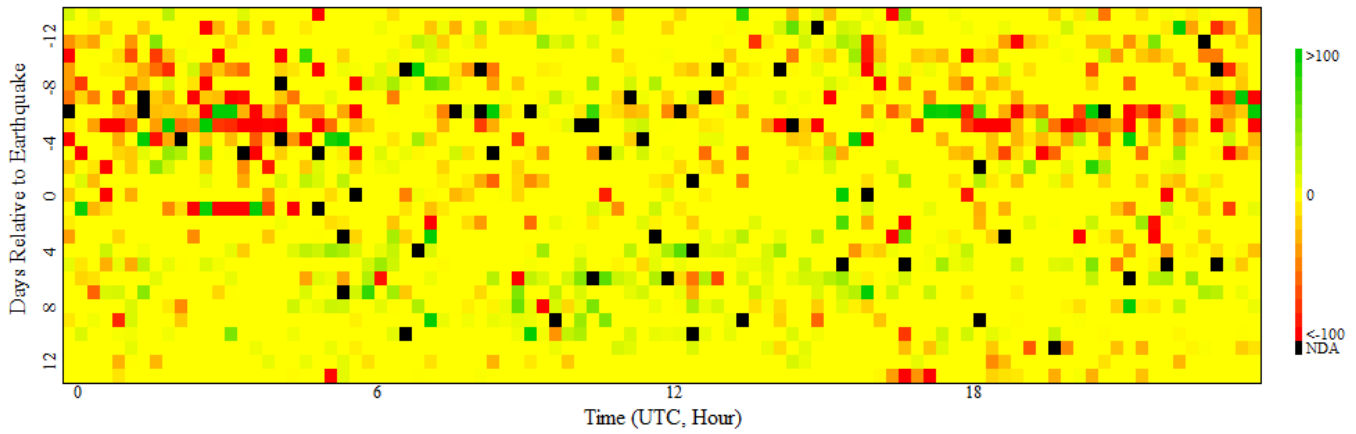

Figure 2. Heat map of the averages of TEC anomaly rates taken from ionosondes located in earthquake preparation zone in earthquakes greater than 6 Mw that occurred in the European continent between 2010-2020. Anomaly rates are shown in colors ranging from red to green as shown in the key, and missing values are shown in black. The rows show the days relative to the earthquake where 0 is the day of the earthquake and the columns show the hours.

In addition, examining the earthquakes occurring in similar regions, during geomagnetic storms of similar magnitudes and different intensities, will make a great contribution to the understanding of the effect of geomagnetic storms on earthquake anomalies.

5. Acknowledgements

We are very grateful to the providers of all the data used in this work for making their data available. Data used in this work were obtained from the Lowell GIRO Data Center giro.uml.edu, the Goddard Space Flight Center omniweb.gsfc.nasa.gov/, the Helmholtz Center Potsdam - GFZ German Research Center for Geosciences www.gfz-potsdam.de/, and the World Data Center for Geomagnetism, Kyoto wdc.kugi.kyoto-u.ac.jp/. The authors would like to thank M. Kıyami Erdim for his supports in writing the code. This study was supported within the scope of TÜBİTAK BİDEB 2209-A - University Students Research Projects Support Program (Project No: 1919B012004244).

References

[1] R.S. Leonard, and R.A. Barnes., "Observation of ionospheric disturbances following the Alaska earthquake," Journal of Geophysical Research, 70(5), 1965, pp.1250–1253, doi: 10.1029/jz070i005p01250.

[2] Z. Fuying, W. Yun, Z. Yiyan, and L. Jian, "A statistical investigation of pre-earthquake ionospheric TEC anomalies", Geodesy and Geodynamics, 2. 2011, pp.61-65, Geodynamics, 2. Doi: 10.3724/SP.J.1246.2011.00061.

[3] S. Pulinets, "Low-latitude atmosphere-ionosphere effects initiated by strong earthquakes preparation process", Int. J. Geophys., (131842), 2012, pp.1–14.

[4] S. Pulinets, and D. Davidenko, "Ionospheric precursors of earthquakes and Global Electric Circuit", Adv. Space Res., 53, 2014, pp.709–723.

[5] J. Guo, W. Li, H. Yu, Z. Liu, C. Zhao and Q. Kong., "Impending ionospheric anomaly preceding the Iquique Mw8.2 earthquake in Chile on 2014 April 1," Geophys. J. Int. 203, 2015, pp.1461–1470 doi: 10.1093 /gji/ggv376

[6] L.P. Dobrovolsky, S.I. Zubkov, and V.I. Miachkin, "Estimation of the size of earthquake preparation zones", Pure Appl. Geophys. 117 (5), 1979, pp.1025–1044 doi: 10.1007/BF00876083.

[7] B.W. Reinisch,and I.A. Galkin, "Global Ionospheric Radio Observatory (GIRO)", Earth Planets, and Space, 63, 2011, pp. 377-381 doi: 10.5047/eps.2011.03.001, 2011.

[8] K. Rawer, "Wave Propagation in the Ionosphere" Kluwer Acad.Publ., Dordrecht 1993, ISBN 0-7923-0775-5.

[9] J.Y. Liu, Y.I. Chen, Y.J. Chuo, & C.S. Chen, "A statistical investigation of pre-earthquake ionospheric anomaly", J. Geophys. pic. 111,2006, A05304, doi:10.1029/2005JA011333.